Bioelectronics

DOI: 10.1002/anie.201106136

A Photo-Thermal-Electrical Converter Based On Carbon Nanotubes for Bioelectronic Applications**

Eijiro Miyako, Chie Hosokawa, Masami Kojima, Masako Yudasaka, Ryoji Funahashi, Isao Oishi, Yoshihisa Hagihara, Mototada Shichiri, Mizuki Takashima, Keiko Nishio, and Yasukazu Yoshida*

There is currently substantial interest in creating bioelectronic devices that can be implanted in and attached to humans for sensing and control of organs and internal systems in order to prolong and improve the quality of life.[1–4] Herein we report a new type of implantable bioelectronic device that is operated by laser irradiation from outside the body. Carbon nanotubes (CNTs), which absorb laser light and transform it to thermal energy with high efficiency, are key in the design of this device; the thermal energy is further converted into electrical power with a Seebeck device. The CNT-based photo-thermal-electrical (PTE) converter is unique and has potential in practical use as it can be simply operated by laser irradiation, and can be easily removed or replaced as it is embedded near the skin.

Among several photothermally active nanomaterials, CNTs are of particular interest because of their extraordinarily high efficiency of photothermal energy conversion and high light-absorption cross-section in a wavelength range that can be transmitted through living tissue (diagnostic window: 650–1100 nm).[5] The photothermal energy conversion of CNTs is effective in various biological applications.[6–19] It is well known that gold nanoparticles also have photothermal properties, but CNTs can be more effectively heated at various wavelengths because of their strong absorbance over a wide wavelength range.[6] Thermal energy can be converted into electricity by using thermoelectric (TE) conversion devices that utilize the Seebeck effect.[18–20] A PTE energy conversion system that combines TE elements and CNTs is available and can be used in the diagnostic window of living tissues. PTE converters are promising devices for electrical power supply to embedded implantable medical devices. We recently fabricated a PTE converter using CNT gels exposed to 1064 nm laser light, and demonstrated that it generated sufficient electrical energy to power a motor and light-emitting diodes.[18,19] However, the applications of our previous PTE converters were limited to ex vivo electrical power generation. Herein, we demonstrate that 1) a well-dispersed single-walled CNT/poly(dimethylsiloxane) (SWNT–PDMS) composite can be formed, and a novel PTE converter fabricated with a CNT polymer composite can effectively convert the photothermal energy of CNTs into electricity; 2) the PTE converter can supply electrical power for stimulation of electrical activity in physiological tissues, such as a heart muscle of zebrafish (*Danio rerio*) and a sciatic nerve of a frog (*Xenopus laevis*); and 3) the PTE converter was effective in the body of a rat. These results dramatically extend the concept of a PTE converter into new areas and applications.

To prepare the CNT-based PTE converter, we first prepared CNT polymer sheets. We wrapped noncovalent SWNTs with poly(3-hexylthiophene) (P3HT) and dispersed them in PDMS sheets (P3HT–SWNT–PDMS; see Methods in the Supporting Information). The strong tendency of CNTs to aggregate means that they do not generally disperse in solvents or polymer matrices.[21] To obtain uniform dispersions of CNTs in a variety of polymer composites, covalent and noncovalent approaches have been used.[21] However, CNTs can tolerate only a limited number of covalently functionalized sites before their optical and electronic properties change significantly.[21,22] Hence, we employed a P3HT-functionalized SWNT (P3HT–SWNT) complex that is highly dispersible in organic solvents by using a noncovalent approach to uniformly disperse the complex in a PDMS polymer matrix[23] (Figure 1a). PDMS is a very attractive material for the present study because it provides a soft, elastomeric, and biocompatible barrier to the surrounding tissue and associated biofluids.[24] The prepared P3HT–SWNT–PDMS sheets were highly flexible and transparent and did not show SWNT aggregation (Figure 1b). The homogeneous dispersibility of P3HT–SWNT complexes in the PDMS polymer matrix was further confirmed by using optical microscopy, Raman scattering, and visible/near-infrared (Vis/NIR) absorption spectra analyses (see Figure S1 in the Supporting Information). The photothermal effect on

[*] Dr. E. Miyako, Dr. C. Hosokawa, Dr. M. Kojima, Dr. I. Oishi, Dr. Y. Hagihara, Dr. M. Shichiri, M. Takashima, K. Nishio
Health Research Institute (HRI)
National Institute of Advanced Industrial Science and Technology (AIST)
1-8-31 Midorigaoka, Ikeda, 563-0026 (Japan)
Dr. M. Yudasaka
Nanotube Research Center, AIST
Central 5, 1-1-1 Higashi, Tsukuba, 305-8565 (Japan)
Dr. R. Funahashi
Research Institute for Ubiquitous Energy Devices, AIST
1-8-31 Midorigaoka, Ikeda, 563-0026 (Japan)
Dr. Y. Yoshida
HRI, AIST, 2217-14 Hayashi-cho, Takamatsu, 761-0395 (Japan)

[**] This work was supported by a Grant-in-Aid for Young Scientists B (23700568). We are grateful to Jun Akedo and So Baba (Advanced Manufacturing Research Institute, AIST) for fruitful discussions about a TE module. We also thank Meijo Nano Carbon (Japan) for providing the multiwalled carbon nanotubes.

Supporting information for this article is available on the WWW under http://dx.doi.org/10.1002/anie.201106136.

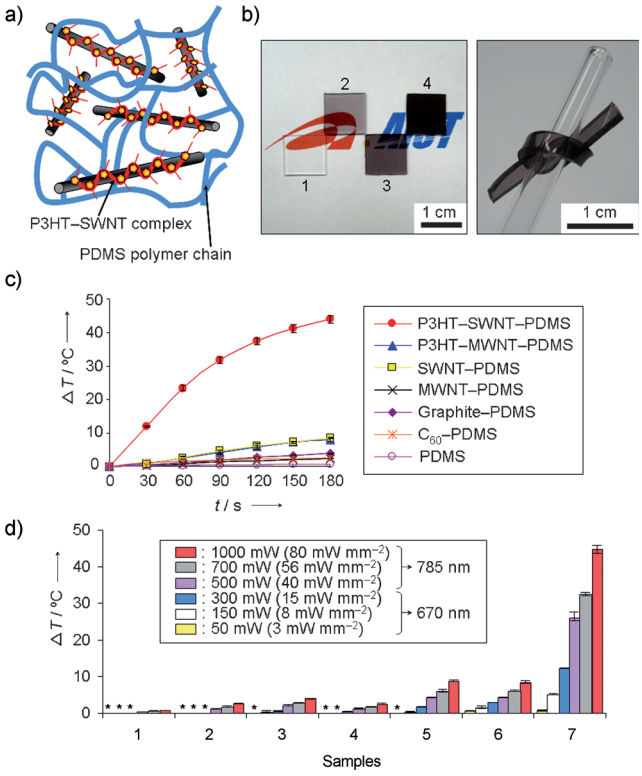

Figure 1. Photothermal properties of the P3HT–SWNT–PDMS composite. a) Schematic illustration of the composite. b) Photographs of the composite. Left: PDMS sheets containing various concentrations of P3HT–SWNT complex; 1) 0 mg mL^{-1}, 2) 0.15 mg mL^{-1}, 3) 0.3 mg mL^{-1}, and 4) 0.6 mg mL^{-1} (the red and blue features are not related to the composites), and right: high flexibility of the composite. c) Temperature increases of various carbon material/PDMS composites under continuous 1064 nm laser irradiation at 1000 mW (ca. 318 mW mm^{-2}). d) Photoinduced temperature elevation in the composites at various laser powers (50, 150, 300, 500, 700, and 1000 mW; ca. 3, 8, 15, 40, 56, and 80 mW mm^{-2}, respectively); 1) PDMS, 2) C_{60}–PDMS, 3) graphite–PDMS, 4) MWNT–PDMS, 5) SWNT–PDMS, 6) P3HT–MWNT–PDMS, and 7) P3HT–SWNT–PDMS. * = Not determined because the temperature did not increase.

P3HT–SWNT–PDMS composites of body-transmissible laser irradiation[7,8] (wavelengths: 670 nm and 785 nm) is also shown (Figure 1c,d). Under laser irradiation, the temperature of the P3HT–SWNT–PDMS composite increases significantly with the irradiation time and power relative to other carbon material/PDMS composites, such as PDMS-encapsulated P3HT-functionalized multiwalled CNTs (P3HT–MWNT–PDMS), nonfunctionalized SWNT–PDMS, PDMS-encapsulated MWNTs (MWNT–PDMS), and PDMS-encapsulated graphite (graphite–PDMS). PDMS-encapsulated buckminsterfullerene (C_{60}–PDMS) and control PDMS composites (without carbon materials) show almost no temperature increases (Figure 1c,d). The high photothermal conversion of P3HT–SWNT–PDMS arises from the high photothermal conversion efficiency of CNTs.[6–19] In addition, well-dispersed SWNTs in P3HT–SWNT–PDMS have a large surface area that absorbs laser light effectively[10] (see Figure S1 in the Supporting Information). P3HT-functionalized MWNTs (P3HT–MWNT) are also well-dispersed in the PDMS polymer matrix, as are P3HT–SWNT complexes (see Figure S2 in the Supporting Information). However, the concentration of MWNTs in the PDMS polymer matrix is about one-quarter of the concentration of SWNTs in PDMS because functionalization with P3HT results in a low dispersability of MWNTs (see Methods and Figure S3 in the Supporting Information). Hence, the temperature increase of P3HT–MWNT–PDMS is lower than that of P3HT–SWNT–PDMS because small amounts of P3HT–MWNT complexes in PDMS have not enough photothermic power to heat the polymer matrix. These results confirm that SWNT complexes were efficient in the polymer matrix as powerful laser-triggered nanoheaters. Incidentally, pristine C_{60} is known to have no photothermal properties.[25]

P3HT–SWNT–PDMS PTE converters (of which type 1 is the smallest) were subsequently manufactured (Figure 2a), and their PTE efficacy was evaluated (Figure 2b and see Figure S6 in the Supporting Information). A Seebeck TE converter with a commercially available bismuth telluride module was used for this study as it has a high TE conversion

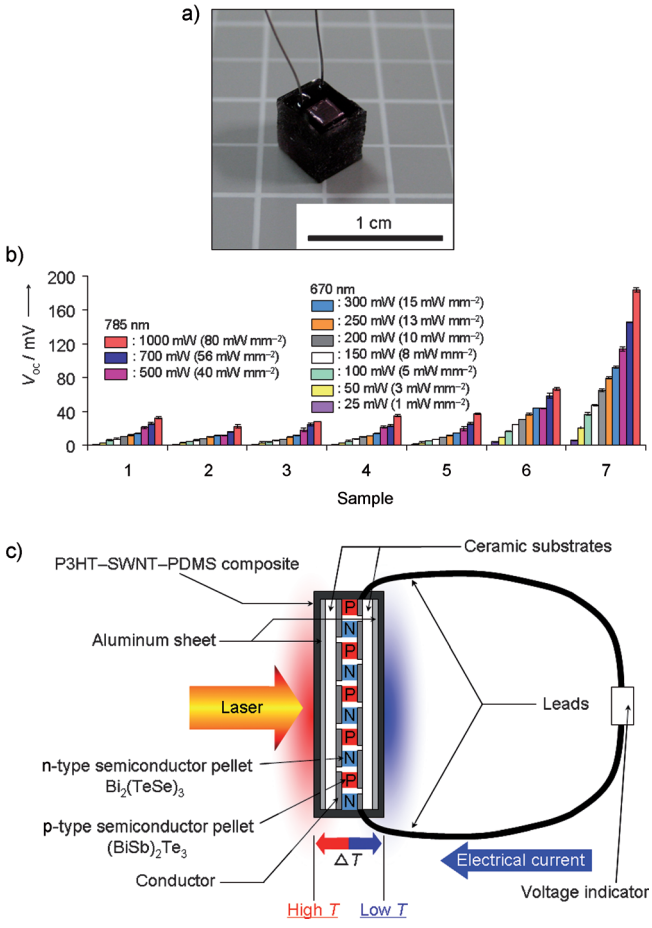

Figure 2. PTE conversion. a) Photograph of the P3HT–SWNT–PDMS PTE converter. b) Open-circuit voltage of PTE converters at various laser powers (25, 50, 150, 300, and 1000 mW; ca. 3, 8, 15, and 80 mW mm^{-2}, respectively); 1) PDMS, 2) C_{60}–PDMS, 3) graphite–PDMS, 4) MWNT–PDMS, 5) SWNT–PDMS, 6) P3HT–MWNT–PDMS, and 7) P3HT–SWNT–PDMS. c) Schematic illustration of PTE conversion.

efficiency over a wide temperature range.[18–20] The carbon material/PDMS composites were attached to the module substrate (see Methods and Figure S7 in the Supporting Information). The PTE conversion mechanism is illustrated in Figure 2c. The p–n junctions on the left-hand side were heated by the photoactivated P3HT–SWNT–PDMS composite, whereas those on the right-hand side were air-cooled. The heat flow across the p–n junctions generated an electrical current through the Seebeck effect.[18–20] The open-circuit voltages (V_{oc}) of the P3HT–SWNT–PDMS PTE converter increased remarkably with increasing laser power (Figure 2b, 7); this performance was superior to the performance of the other carbon-based PTE converters (Figure 2b, 1–6). The electrical current (I) of the P3HT–SWNT–PDMS PTE converter also increased with increasing laser power, as well as the V_{oc} value (see Figure S6 in the Supporting Information). The I values were calculated by using Ohm's law.[18,19] The maximum electrical power (P_{max}) of the P3HT–SWNT–PDMS converter is calculated to be about 3200 μW by using Equation (1)[26] under 785 nm laser irradiation at 1000 mW (laser power density ≈ 80 mW mm^{-1}; see Figure S6 in the Supporting Information):

$$P_{max} = V_{oc}^2/(4R_i) \quad (1)$$

where R_i is the internal resistance of the module ($R_i \approx 2.7\ \Omega$). In addition, the electrical performances of three differently sized PTE converters were investigated (type 1, type 2, and type 3; see Methods and Figure S8 in the Supporting Information). The smallest PTE converter (type 1) showed the highest electrical values ($V_{oc} = 94$ mV, $I = 35$ mA, $P_{max} = 811$ μW). The type 1 converter was effectively heated by laser light because the converter size (ca. 4.0 mm × 4.0 mm × 4.4 mm) fitted the laser spot diameter (ca. 4–5 mm; see Figure S8b in the Supporting Information). In addition, the effect of P3HT–SWNT concentrations on the electrical performance of the converter were studied (see Figure S9 in the Supporting Information). As the P3HT–SWNT complex concentration increased, the electrical performance (V_{oc}, I, and P_{max}) of the PTE converter increased. Furthermore, we did not observe serious damage of the P3HT–SWNT–PDMS PTE converter, even under high-power laser irradiation over a long period (785 nm, 1000 mW (80 mW mm^{-2}), > 12 h); this observation is probably a result of the high thermal stability of the PDMS molecule[16] (see Figure S10 in the Supporting Information). It is noted that the electrical capability of the PTE converter was also not affected by this laser irradiation. These results clearly demonstrate that the PTE converter generates sufficient electrical energy and has high photothermal stability.

The main purpose of this study is to remotely control electrical energy generation by laser light that can be transmitted through living tissue in order to target various bionic applications. For our first system, we used laser-triggered remote electrical stimulation for a *Danio rerio* heart (Figure 3a, b). Tungsten microneedle electrodes connected to the PTE converter (type 3) were inserted into a ventricle of the heart (Figure 3a). When laser irradiation (1064 nm, 1000 mW (ca. 318 mW mm^{-2})) was commenced, apparent

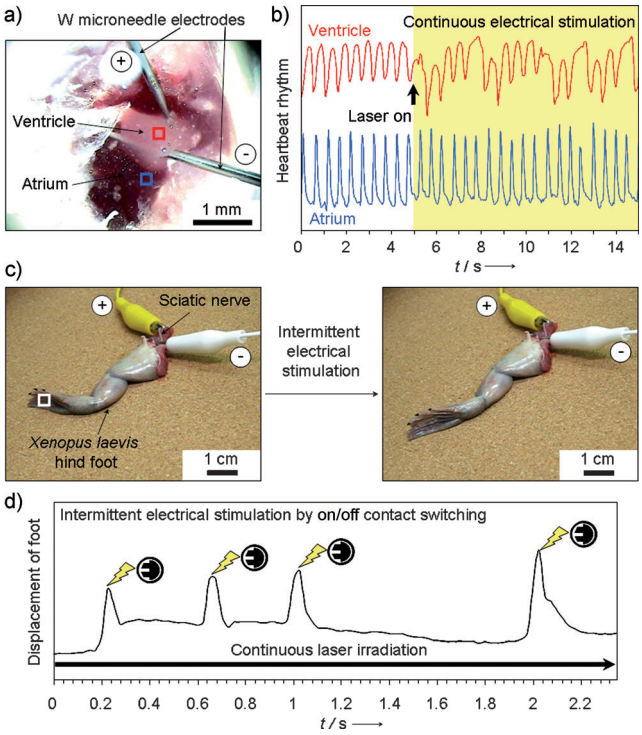

Figure 3. Electrical stimulations of heart and nerves by the P3HT–SWNT–PDMS PTE converter. a, b) Laser-triggered remote electrical stimulation of the heartbeat of *Danio rerio*. Red and blue squares indicate the locations where the movements of ventricle and atrium, respectively, were analyzed. c, d) Laser-driven remote electrical stimulation of sciatic nerve of *Xenopus laevis*. White squares indicate the location where the movements of the hind foot were analyzed. Experimental conditions: wavelength = 1064 nm, laser power = 1000 mW (ca. 318 mW mm^{-2}).

arrhythmia of the ventricle (ventricular fibrillation) was immediately observed, although the atrial rhythm was unchanged (see Figure 3b, and see Video 1 in the Supporting Information). The electrically stimulated heart slowly stopped within 5 min. The second example is the electrical stimulation of a sciatic nerve of *Xenopus laevis* using the PTE converter (type 3; Figure 3c, d). Conducting leads were connected to the PTE converter, which was then inserted into the white corded sciatic nerve of the hind foot of *Xenopus laevis* (Figure 3c). We observed twitching that was driven by intermittent electrical stimulation (on/off contact switching of the leads) under continuous 1064 nm laser irradiation at 1000 mW (ca. 318 mW mm^{-2}; see Figure 3d and see Video 2 in the Supporting Information). In control experiments using other PTE converters based on carbon material/PDMS composites and PDMS, the same laser irradiation caused neither ventricular fibrillation in *Danio rerio* nor hind-foot twitching in *Xenopus laevis*. Thus, we consider these dynamic responses to be due to the excitability of ion channel protein molecules in the ventricle[27] and sciatic nerve[28] activated by electricity (ca. 100 mV) from the P3HT–SWNT–PDMS PTE converter (see Figure S11 in the Supporting Information). These results clearly indicate that electrical activities of muscles and nerves can be remotely stimulated by PTE conversion.

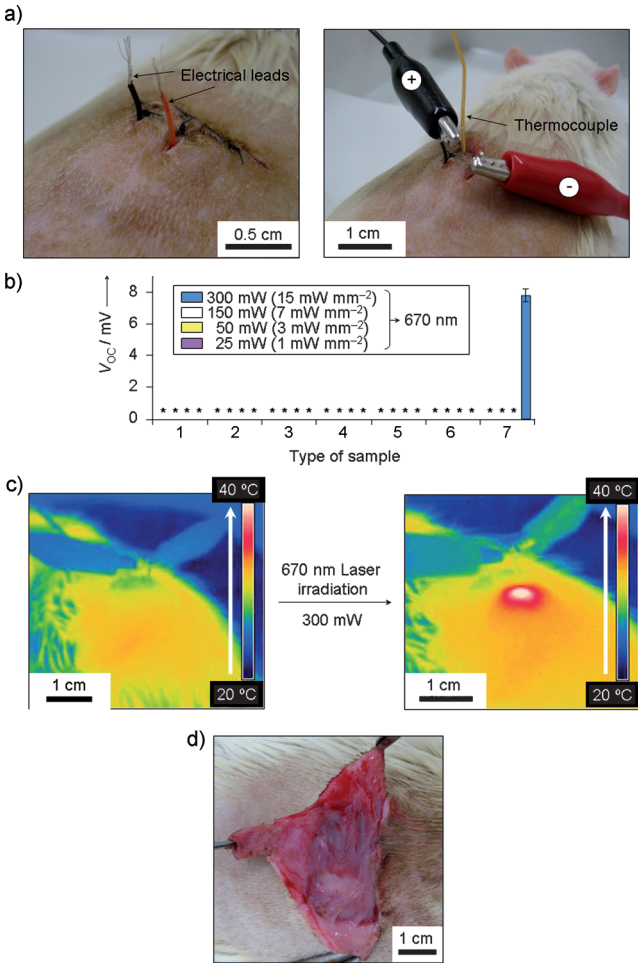

Figure 4. In vivo PTE conversion. a) Photographs of PTE converter implanted in a rat. b) Voltage measurements by laser-driven in vivo PTE conversion (wavelength = 670 nm) at various laser power levels (25, 50, 150, and 300 mW; ca. 1, 3, 8, and 15 mW mm^{-2}, respectively); 1) PDMS, 2) C_{60}–PDMS, 3) graphite–PDMS, 4) MWNT–PDMS, 5) SWNT–PDMS, 6) P3HT–MWNT–PDMS, 7) P3HT–SWNT–PDMS. * = Not determined because no voltages were detected. c) Thermographic measurements on the body's surface with 670 nm laser driven PTE converters at 300 mW. d) Anatomical photograph of PTE implant region after 670 nm laser irradiation at 300 mW (ca. 15 mW mm^{-2}) over 1 h.

Finally, we investigated in vivo electrical power generation by PTE conversion in the body of a rat (Figure 4 and see Figure S12 in the Supporting Information). The implanted PTE converter (type 3) under the skin of a rat was barely noticeable because the converter was so small (ca. 10 mm × 10 mm × 4.4 mm; Figure 4a, left). We monitored V_{oc} by using a 670 nm laser at various power levels (25–300 mW (ca. 1–15 mW mm^{-2}); Figure 4a, right). Only the P3HT–SWNT–PDMS PTE converter (Figure 4b, 7) generates electricity (V_{oc} ≈ 8 mV) by 300 mW laser irradiation (ca. 15 mW mm^{-2}; Figure 4b). The P_{max} value of the PTE converter is estimated to be about 6 μW according to Equation (1).[26] The electrical performance of our converter was improved when two converters connected in series were irradiated by two laser beams (see Figure S13 in the Supporting Information). The temperature differences (ΔT) in the body were investigated by using a thermocouple inserted under the converter; only the P3HT–SWNT–PDMS converter produced increasing temperatures after 150 mW and 300 mW laser irradiation (8 and 15 mW mm^{-2}, respectively; see Figure S14a in the Supporting Information). In addition, we observed a temperature difference at the body surface by using infrared thermography (Figure 4c and see Figure S14b in the Supporting Information). After 670 nm laser irradiation at 300 mW (ca. 15 mW mm^{-2}), the approximate temperature of the rat's body surface increased from 30 °C to 40 °C when the P3HT–SWNT–PDMS PTE converter was used. The highest temperature difference of the body surface was obtained when the P3HT–SWNT–PDMS PTE converter received 300 mW laser irradiation (see Figure S14b in the Supporting Information). No effects such as burns or inflammation appeared near the PTE converter after laser irradiation (> 30 min) of the rat under general anesthesia (Figure 4d). Furthermore, the implanted P3HT–SWNT–PDMS PTE converter has no toxicity, at least for 1 month (see Figure S15 and Table S1 in the Supporting Information). We conclude that the PTE conversion safely and effectively causes a top-to-bottom temperature gradient by using the powerful photothermal properties of well-dispersed CNT molecules in the polymer matrix, and thus resulting in significant in vivo electrical generation.

In conclusion, we have successfully developed a novel PTE converter in which a PDMS composite encapsulates a uniformly dispersible P3HT–SWNT complex; the converter enables remote electrical stimulation of physiological tissue such as muscles and nerves under laser irradiation. In addition, electrical power was successfully remotely generated in a living body by using this converter and a laser that can penetrate living tissue. To the best of our knowledge, this is the first demonstration of remote control of physiological tissue activities and in vivo electrical power generation through a new type of PTE converter that exploits the powerful photothermal properties of CNTs. This study also provides a new mechanism for designing various bioelectronic devices, such as a power source for the stimulation of living tissues,[27,28] a sensing material for optical biotelemetry,[29] and a power supply system for implantable medical devices.[1–4]

Received: August 30, 2011
Published online: October 26, 2011

Keywords: bioelectronics · energy conversion · nanotechnology · nanotubes · semiconductors

[1] A. Darwish, A. E. Hassanien, *Sensors* **2011**, *11*, 5561–5595.
[2] S. K. Talwar, S. Xu, E. S. Hawley, S. A. Weiss, K. A. Moxon, J. K. Chapin, *Nature* **2002**, *417*, 37–38.
[3] P. Cinquin et al., *PLoS ONE* **2010**, *5*, e10476–e10472. See the Supporting Information for full reference.
[4] Z. Li, G. Zhu, R. Yang, A. C. Wang, Z. L. Wang, *Adv. Mater.* **2010**, *22*, 2534–2537.
[5] K. König, *J. Microsc.* **2000**, *200*, 83–104.
[6] J. T. Robinson, K. Welsher, S. M. Tabakman, S. P. Sherlock, H. Wang, R. Luong, H. Dai, *Nano Res.* **2010**, *3*, 779–793.

[7] N. W. Shi Kam, M. O'Connell, J. A. Wisdom, H. Dai, *Proc. Natl. Acad. Sci. USA* **2005**, *102*, 11600 – 11605.
[8] H. K. Moon, S. H. Lee, H. C. Choi, *ACS Nano* **2009**, *3*, 3707 – 3713.
[9] M. Zhang, T. Murakami, K. Ajima, K. Tsuchida, A. S. D. Sandanayaka, O. Ito, S. Iijima, M. Yudasaka *Proc. Natl. Acad. Sci. USA* **2008**, *105*, 14773 – 14778.
[10] E. Miyako, H. Nagata, K. Hirano, T. Hirotsu, *Angew. Chem.* **2008**, *120*, 3666 – 3669; *Angew. Chem. Int. Ed.* **2008**, *47*, 3610 – 3613.
[11] E. Miyako, H. Nagata, K. Hirano, T. Hirotsu, *Adv. Mater.* **2009**, *21*, 2819 – 2823.
[12] E. Miyako, H. Nagata, K. Hirano, T. Hirotsu, *Lab Chip* **2009**, *9*, 788 – 794.
[13] E. Miyako, T. Itho, Y. Nara, T. Hirotsu, *Chem. Eur. J.* **2009**, *15*, 7520 – 7525.
[14] E. Miyako, H. Nagata, K. Hirano, T. Hirotsu, *Small* **2008**, *4*, 1711 – 1715.
[15] E. Miyako et al., *Nanotechnology* **2007**, *18*, 475103.
[16] E. Miyako, H. Nagata, K. Hirano, K. Sakamoto, Y. Makita, K. Nakayama, T. Hirotsu, *Nanotechnology* **2008**, *19*, 075106.
[17] E. Miyako, H. Nagata, K. Hirano, Y. Makita, T. Hirotsu, *Chem. Phys. Lett.* **2008**, *456*, 220 – 222.
[18] E. Miyako, H. Nagata, R. Funahashi, K. Hirano, T. Hirotsu, *ChemSusChem* **2009**, *2*, 740 – 742.
[19] E. Miyako, H. Nagata, R. Funahashi, K. Hirano, T. Hirotsu, *ChemSusChem* **2009**, *2*, 419 – 422.
[20] L. E. Bell, *Science* **2008**, *321*, 1457 – 1461.
[21] P. M. Ajayan, J. M. Tour, *Nature* **2007**, *447*, 1066 – 1068.
[22] M. S. Strano, C. A. Dyke, M. L. Usrey, P. W. Barone, M. J. Allen, H. Shan, C. Kittrell, R. H. Hauge, J. M. Tour, R. E. Smalley, *Science* **2003**, *301*, 1519 – 1522.
[23] J. Geng, B.-S. Kong, S. B. Yang, S. C. Youn, S. Park, T. Joo, H.-T. Jung, *Adv. Funct. Mater.* **2008**, *18*, 2659 – 2665.
[24] R.-H. Kim et al., *Nat. Mater.* **2010**, *9*, 929 – 937. See the Supporting Information for full reference.
[25] V. Krishna, N. Stevens, B. Koopman, B. Moudgil, *Nat. Nanotechnol.* **2010**, *5*, 330 – 334.
[26] R. Funahashi, S. Urata, K. Mizuno, T. Kouuchi, M. Mikami, *Appl. Phys. Lett.* **2004**, *85*, 1036 – 1038.
[27] D. J. Dosdall, V. G. Fast, R. E. Ideker, *Annu. Rev. Biomed. Eng.* **2010**, *12*, 233 – 258.
[28] X. Navarro, T. B. Krueger, N. Lago, S. Micera, T. Stieglitz, P. Dario, *J. Peripher. Nerv. Syst.* **2005**, *10*, 229 – 258.
[29] H. P. Kimmich, *Biotel. Pat. Monit.* **1982**, *9*, 129 – 143.

